Supporting Information

Chainlike Mesoporous SnO_2 as a Well-Performing Catalyst for Electrochemical CO_2 Reduction

Katarzyna Bejtka [*,†], *Juqin Zeng* [*,†], *Adriano Sacco* [†], *Micaela Castellino* [‡], *Simelys Hernández* [†], *M. Amin Farkhondehfal* [†], *Umberto Savino* [†,‡], *Simone Ansaloni* [‡], *Candido F. Pirri* [†,‡] *and Angelica Chiodoni* [†]

[†] Center for Sustainable Future Technologies @POLITO, Istituto Italiano di Tecnologia, Via Livorno 60, 10144 Turin, Italy

[‡] Department of Applied Science and Technology, Politecnico di Torino, Corso Duca degli Abruzzi 24, 10129 Turin, Italy

*E-mail: Katarzyna.Bejtka@iit.it, *E-mail: Juqin.Zeng@iit.it

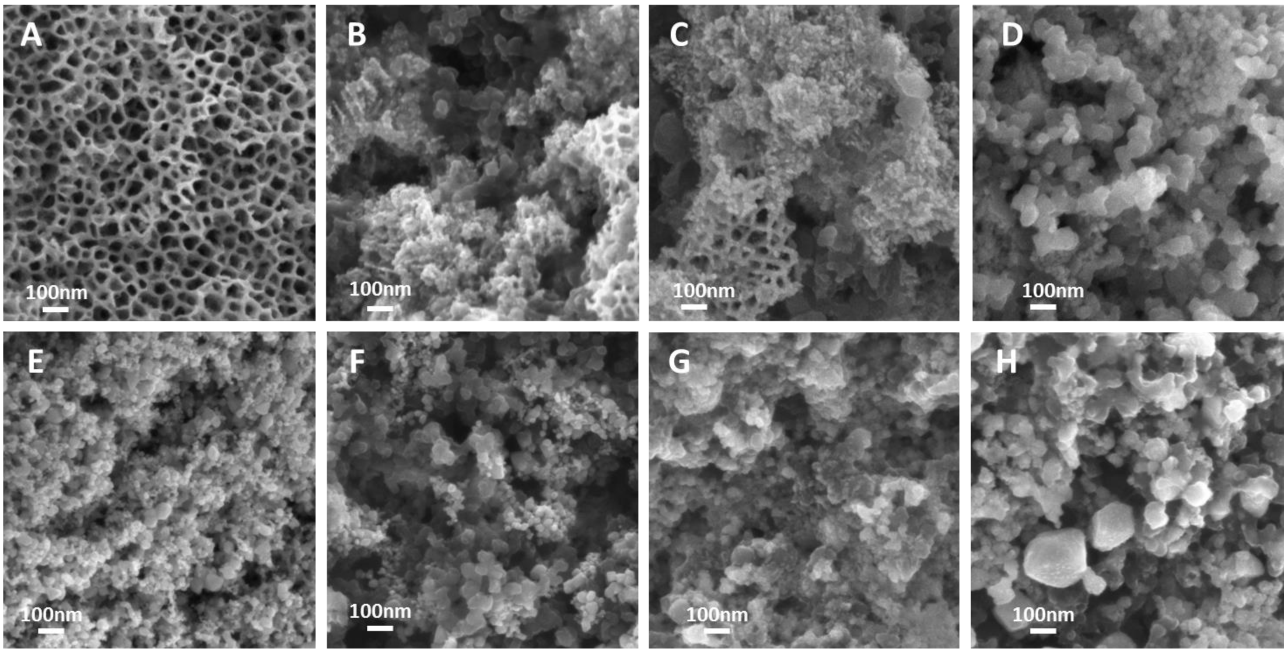

Figure S1 Top view FESEM images of the (a) as-grown SnO_2,(b) as-prepared electrode SnO_2-anod, (c) SnO_2-anod electrode reduced for 20min and (d) tested SnO_2-anod electrode, (e) commercial SnO_2, (f) as-prepared electrode SnO_2-comm, (g) SnO_2-comm electrode reduced for 20min and (h) tested SnO_2-comm electrode. All images are shown at the same magnification.

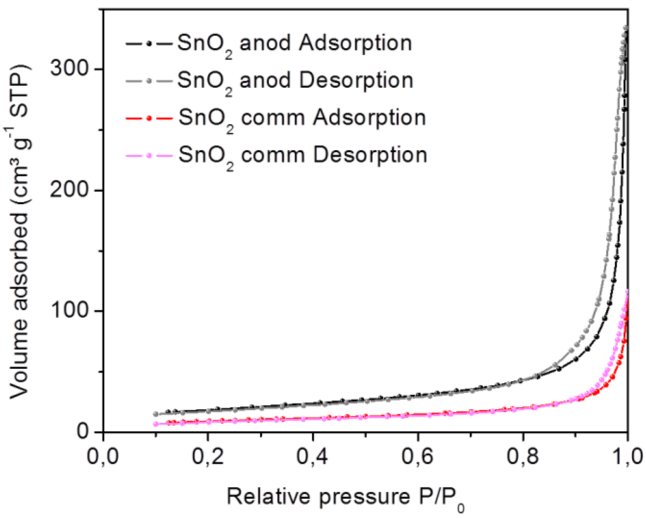

Figure S2 N_2 adsorption/desorption isotherms for SnO_2 prepared via anodic oxidation and commercial.

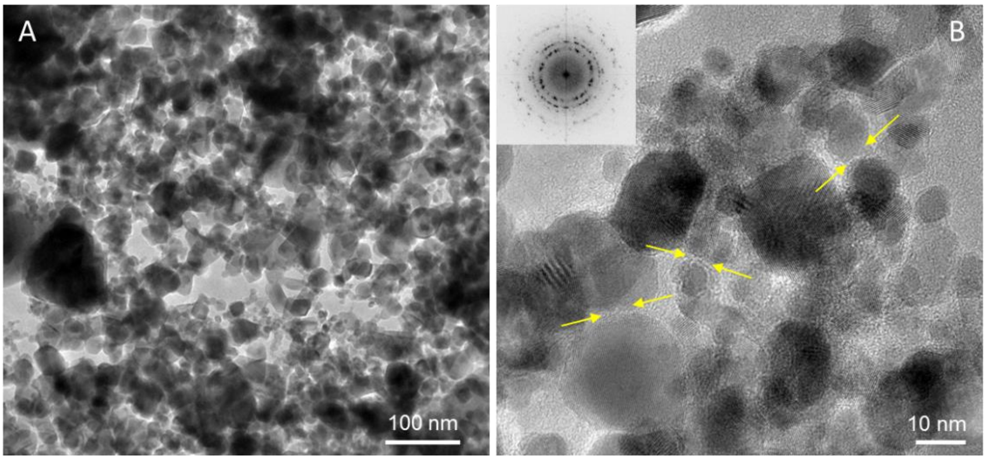

Figure S3 TEM image at two different magnification of the commercial SnO_2. In the inset the FFT of picture (b) is also reported.

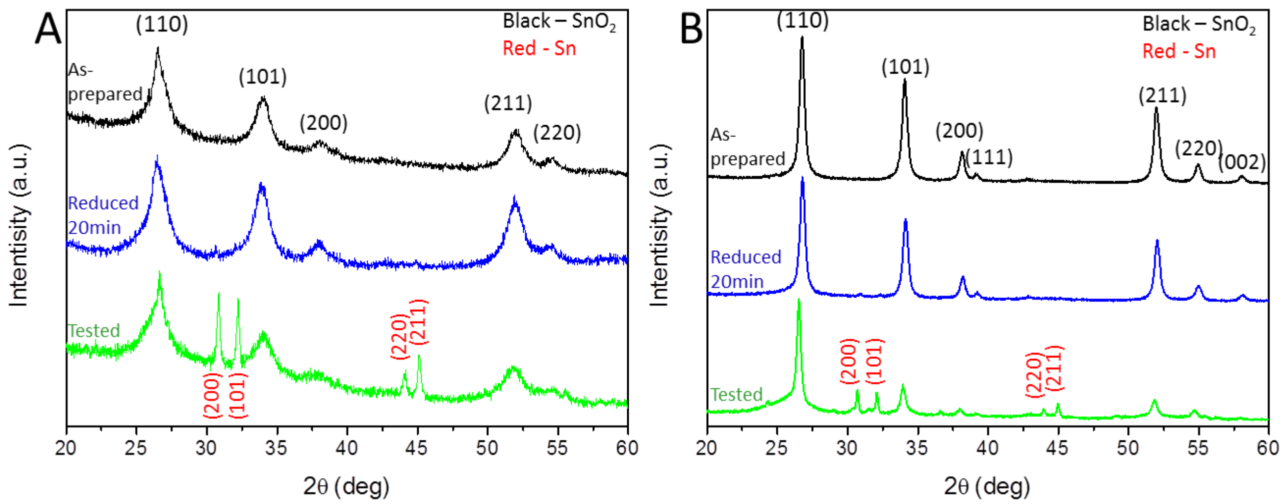

Figure S4 XRD patterns of (a) SnO_2-anod and (b) SnO_2-comm electrodes (as-prepared, reduced for 20min and tested).

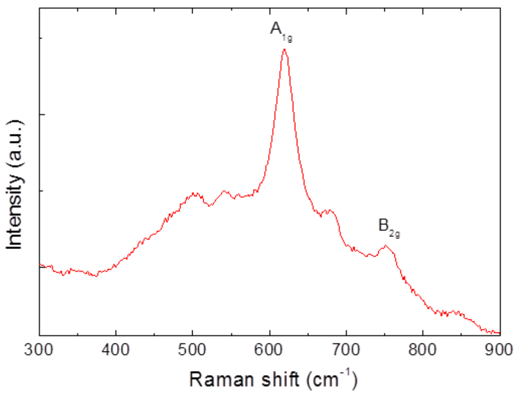

Figure S5 Raman spectrum of as-prepared SnO_2-anod electrode.

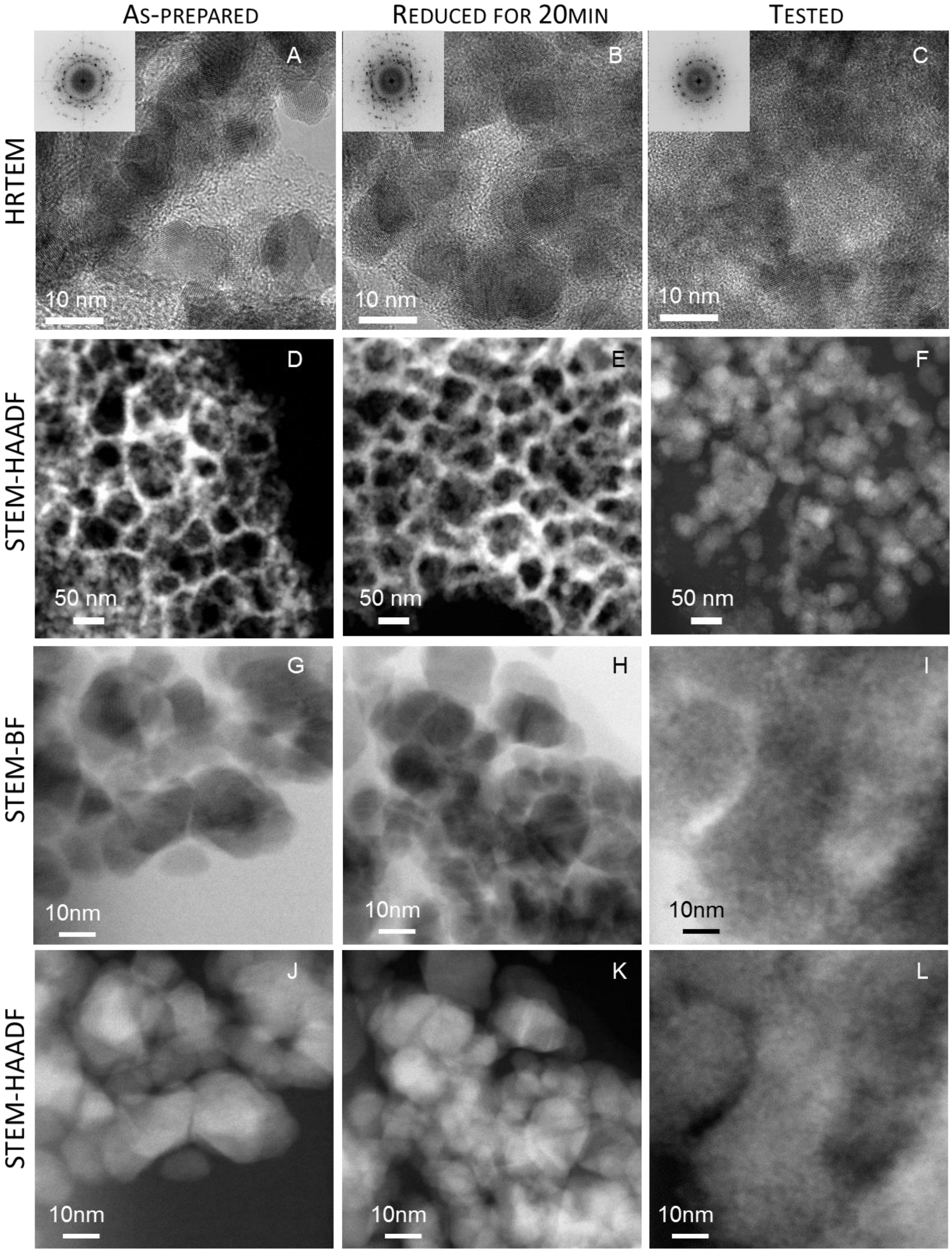

Figure S6 TEM study of the crystals evolution of the SnO_2-anod, including the as-prepared, reduced for 20 minutes and long term tested material. In the rows the following images are shown: HRTEM with FFT (of the shown area) in the inset, low magnification HAADF-STEM image, high magnification BF-STEM and HAADF-STEM.

The double-layer capacitance (C_{dl}) values of the SnO_2-comm, SnO_2-anod and Sn foil electrodes are evaluated by cyclic voltammetry (CV) at various scan rates in a potential range between -0.29 V and -0.39 V. The geometric current densities are plotted against the scan rates, and the slope of the linear fitting quantifies the double-layer capacitance C_{dl}.

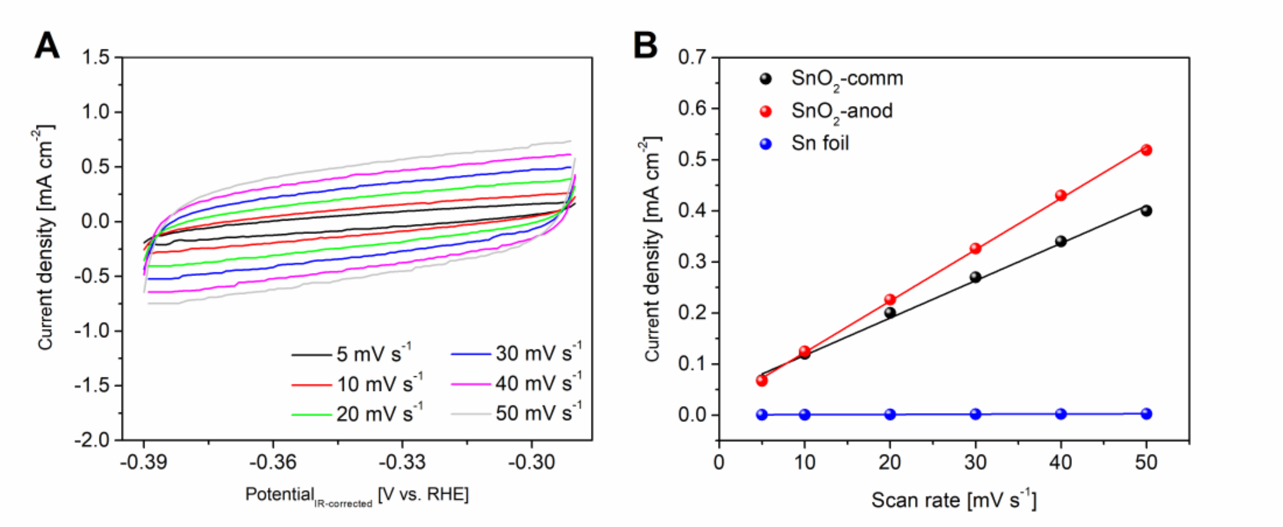

Figure S7 Determination of double-layer capacitance for various electrodes in CO_2-saturated 0.1 M KHCO3: (a) representing CVs on SnO_2-anod electrode; (b) Capacitance values calculated from the slopes of current densities vs. scan rate.

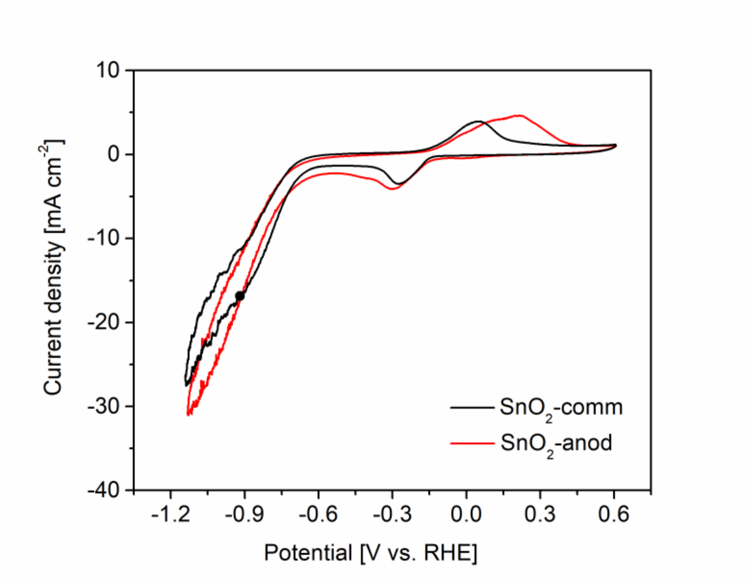

Figure S8 Comparison of the voltammograms of SnO_2-comm and SnO_2-anod in the CO_2-saturated electrolyte.

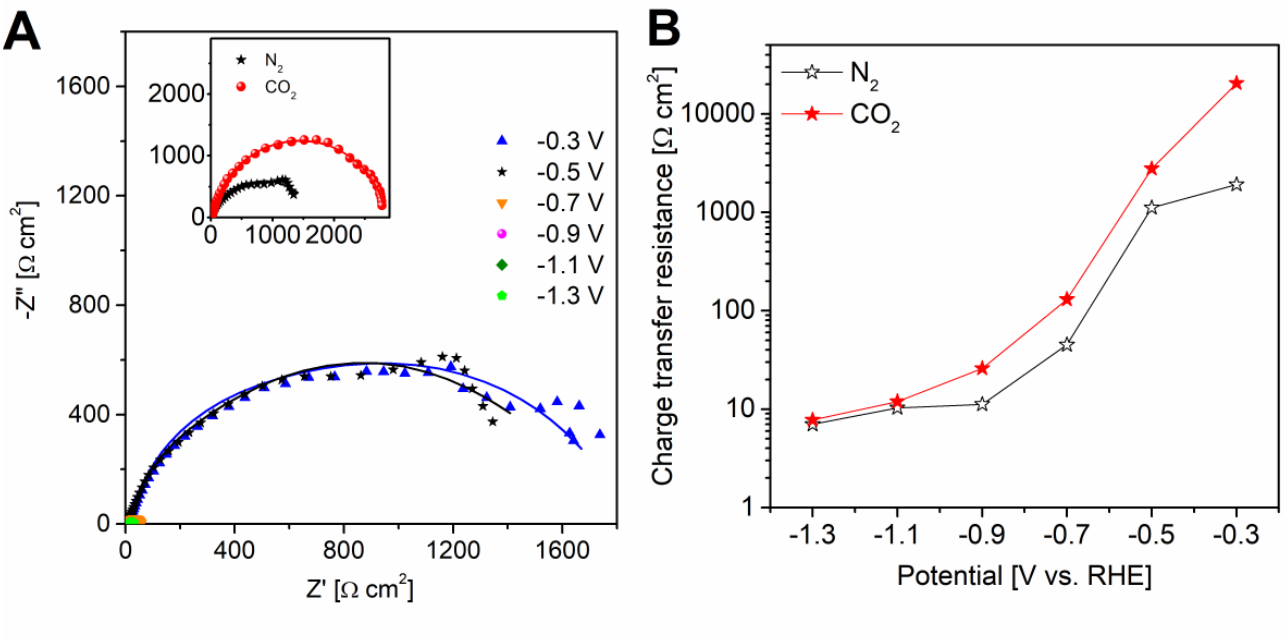

Figure S9 EIS analysis on a Sn foil electrode: (a) Nyquist plots obtained in N_2-saturated electrolyte (the points are experimental data, the clines are the curves calculated through fitting. In the inset, the two spectra acquired at -0.5 V in N2- and CO_2-saturated solutions are shown. (b) Charge transfer resistances reported as a function of the potential.

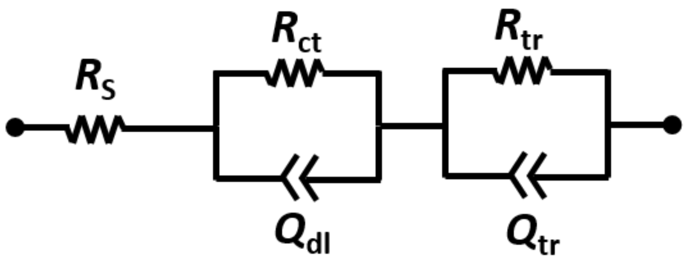

Figure S10 Equivalent circuit used for fitting of EIS data.

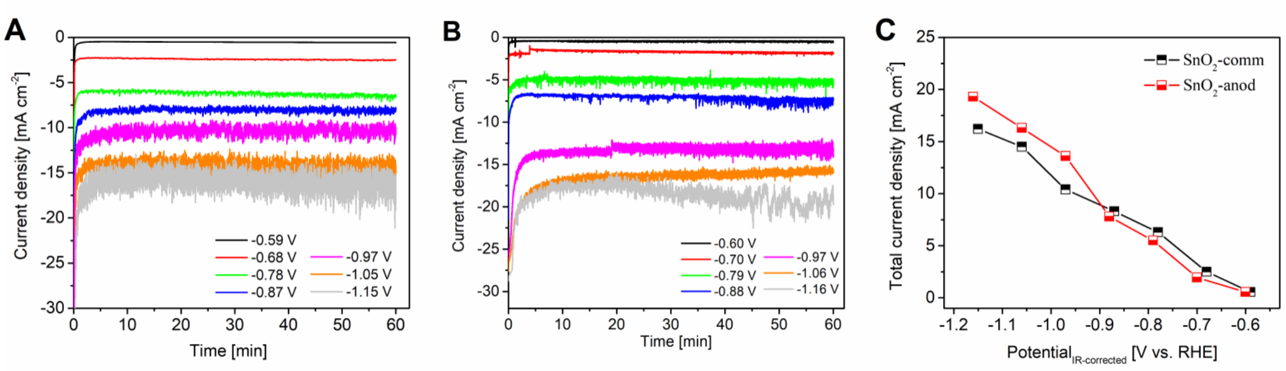

Figure S11 CA measurements carried out in CO_2-saturated 0.1 M $KHCO_3$ aqueous solution at different potentials: (a) SnO_2-comm; (b) SnO_2-anod; (c) Comparison of total current densities on SnO_2-comm and SnO_2-anod electrodes at various potentials.

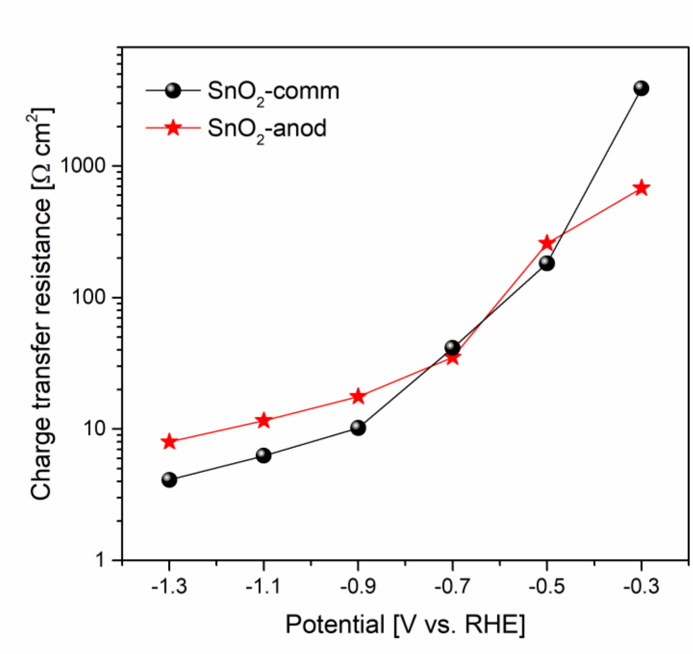

Figure S12 Comparison of charge transfer resistance obtained from EIS on SnO_2-comm and SnO_2-anod electrodes at various potentials.

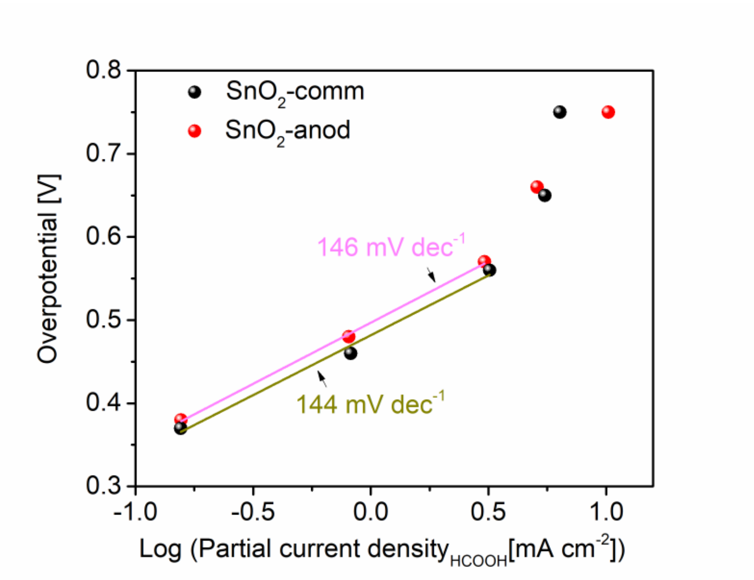

Figure S13 Tafel plot analysis for HCOOH production on SnO_2-comm and SnO_2-anod electrodes.

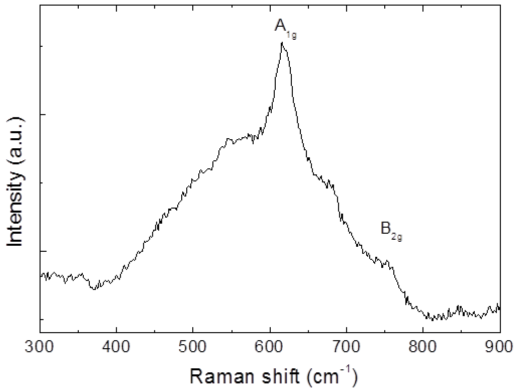

Figure S14 Raman spectrum of tested SnO_2-anod electrode.

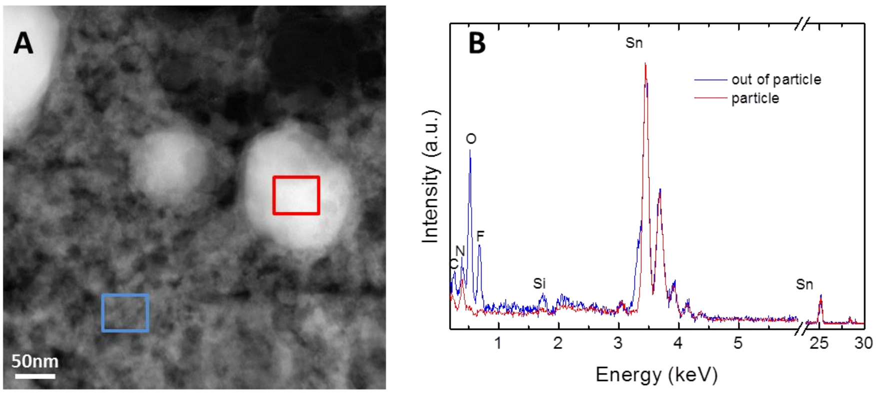

Figure S15 STEM image of the cross-section lamella of tested SnO_2-anod electrode (a) and EDX measurement performed locally in the particle and out of the particle (b).

Table S1 Comparison of electrocatalytic performance for reducing CO_2 to formic acid / formate on tin-based catalysts.

Electrode	Electrolyte	Maximum Faradic Efficiency [%]	Total current (mA cm^{-2})	Ref
Sn/SnO_2 porous hollow fiber	0.1 M $KHCO_3$	82% @-1.,6 V (vs. SCE)	28,6	1
SnO_2 nanosheets/Carbon cloth	0.5 M $NaHCO_3$	87% @ −1.6 V (vs. Ag/AgCl)	48,6	2
SnO_x NPs	0.5 M $KHCO_3$	87% @ −1.6 V (vs. SHE)	14,0	3
Electro deposited Sn	0.1 M $KHCO_3$	91% @ −1.4 V (vs. SCE)	15,0	4
Sn particles	0.5 M $KHCO_3$	73% @ −1.8 V (vs. Ag/AgCl)	13,5	5
SnO_2 nanopowder	0.5 M NaOH	68% @-0.6 V (vs. RHE)	3,5	6
SnO_2/graphene	0.1 M $NaHCO_3$	94% @-1.8 V (vs. SCE)	10,2	7
SnO_2/carbon black	0.1 M $NaHCO_3$	86% @-1.8 V (vs. SCE)	5,4	7
Sn dendrite	0.1 M $KHCO_3$	72% @-1.36 V (vs. RHE)	17,1	8
Sn - Nafion	0.5 M $NaHCO_3$	70% @-1.6 V (vs. NHE)	27,0	9
SnO_2/carbon aerogel	1.0 M $KHCO_3$	76% @ −0.96 V (vs. RHE)	23,5*	10
SnO_2 Porous NWs	0.1 M $KHCO_3$	80% @ -0.8 V (vs. RHE)	6,0	11
SnO_2 NPs	0.1 M $KHCO_3$	58% @ -0.8 V (vs. RHE)	2,4	11
SnO_2 at N-rGO	0.5 M $NaHCO_3$	78% @ -0.8 V (vs. RHE)	21,3	12
SnO_2 nanospheres	0.5 M $KHCO_3$	56% @ -1.1 V (vs. RHE)	6,0*	13
Mmesoporous SnO_2	0.1 M $KHCO_3$	40% @ -0.8 V (vs. RHE)	5.0	14
		40% @ -1.4 V (vs. RHE)	21.3	14
Chain-like mesoporous SnO_2	0.1 M $KHCO_3$	82% @ -1.06 V (vs. RHE)	16,3	This work
		80% @ -1.15 V (vs. RHE)	19.3	This work
SnO2 nanopowder	0.1 M $KHCO_3$	43% @ -1.15 V (vs. RHE)	16.2	This work
		67% @ -0.87 V (vs. RHE)	8.3	This work

* estimated on the basics of information given in the paper

References

(1) Hu H., Gui L., Zhou W., Sun J., Xu J., Wang Q., He B., Zhao L. Partially reduced Sn/SnO_2 porous hollow fiber: A highly selective, efficient and robust electrocatalyst towards carbon dioxide reduction. *Electrochimica Acta* **2018**, 285, 70-77.

(2) Li F., Chen L., Knowles G.P., MacFarlane D.R., Zhang J. Hierarchical Mesoporous SnO_2 Nanosheets on Carbon Cloth: A Robust and Flexible Electrocatalyst for CO_2 Reduction with High Efficiency and Selectivity, *Angew. Chem. Int. Ed*. **2017**, 56, 505-509.

(3) Li Y., Qiao J., Zhang X., Lei T., Girma A., Liu Y., Zhang J. Rational Design and Synthesis of SnO_x Electrocatalysts with Coralline Structure for Highly Improved Aqueous CO_2 Reduction to Formate. *ChemElectroChem* **2016**, 3, 1618 – 1628.

(4) Zhao C.C., Wang J.L. Electrochemical reduction of CO_2 to formate in aqueous solution using electro-deposited Sn catalysts. *Chem. Eng. J*. **2016**, 293, 161–170.

(5) Wang Q., Dong H., Yu H. Fabrication of a novel tin gas diffusion electrode for electrochemical reduction of carbon dioxide to formic acid. *RSC Adv*. **2014**, 4, 59970–59976.

(6) Lee S., Ocon J.D., Son Y., Lee J. Alkaline CO_2 Electrolysis toward Selective and Continuous $HCOO^-$ Production over SnO_2 Nanocatalysts. *J. Phys. Chem. C* **2015**, 119, 4884–4890.

(7) Zhang, S., Kang, P., Meyer, T.J. Nanostructured Tin Catalysts for Selective Electrochemical Reduction of Carbon Dioxide to Formate. *J. Am. Chem. Soc*. **2014**, 136, 1734−1737.

(8) Won D.H., Choi C.H., Chung J.H., Chung M.W., Kim E.H., Woo S.I. Rational Design of a Hierarchical Tin Dendrite Electrode for Efficient Electrochemical Reduction of CO_2. *ChemSusChem* **2015**, 8, 3092–3098.

(9) Surya Prakash G.K., Viva F.A., Olah G.A. Electrochemical reduction of CO_2 over Sn-Nafion coated electrode for a fuel-cell-like device. *J. Power Sources* **2012**, 223, 68–73.

(10) Yu J., Liu H., Song S., Wang Y., Tsiakaras P. Electrochemical reduction of carbon dioxide at nanostructured SnO_2/carbon aerogels: The effect of tin oxide content on the catalytic activity and formate selectivity. *Appl. Catal A, General* **2017**, 545, 159–166.

(11) Kumar B., Atla V., Brian J.P., Kumari S., Nguyen T.Q., Sunkara M., Spurgeon J.M. Reduced SnO_2 Porous Nanowires with a High Density of Grain Boundaries as Catalysts for Efficient Electrochemical CO_2-into-HCOOH Conversion. *Angew. Chem. Int. Ed*. **2017**, 56, 3645 –3649.

(12) Zhang B., Guo Z., Zuo Z., Pan W., Zhang J. The Ensemble Effect of Nitrogen Doping and Ultrasmall SnO_2 Nanocrystals on Graphene Sheets for Efficient Electroreduction of Carbon Dioxide. *Appl. Catal B. Environ*. **2018**, 239, 441–449.

(13) Fu Y., Li Y., Zhang X., liu Y., Zhou X., Qiao J. Electrochemical CO_2 reduction to formic acid on crystalline SnO_2 nanosphere catalyst with high selectivity and stability. Chinese Journal of Catalysis **2016**, 37, 1081–1088.
(14) Ge H., Gu Z., Han P., Shen H., Al-Enizi A. M., Zhang L., Zheng G. J. Mesoporous Tin Oxide for Electrocatalytic CO2 Reduction. *Colloid Interface Sci*. **2018**, 531, 564-569.